Applied Physics Letters

Direct measurement of photocathode time response in a high-brightness photoinjector

Cite as: Appl. Phys. Lett. **120**, 104102 (2022); https://doi.org/10.1063/5.0078927
Submitted: 16 November 2021 • Accepted: 09 February 2022 • Published Online: 08 March 2022

Gregor Loisch, Ye Chen, Christian Koschitzki, et al.

Applied Physics Letters ARTICLE scitation.org/journal/apl

Direct measurement of photocathode time response in a high-brightness photoinjector

Cite as: Appl. Phys. Lett. **120**, 104102 (2022); doi: 10.1063/5.0078927
Submitted: 16 November 2021 · Accepted: 9 February 2022 ·
Published Online: 8 March 2022

Gregor Loisch,[1,a),b)] Ye Chen,[2,b)] Christian Koschitzki,[1] Houjun Qian,[1] Matthias Gross,[1] Adrian Hannah,[3] Andreas Hoffmann,[1] Davit Kalantaryan,[1] Mikhail Krasilnikov,[1] Sven Lederer,[2] Xiangkun Li,[1] Osip Lishilin,[1] David Melkumyan,[1] Laura Monaco,[4] Raffael Niemczyk,[1] Anne Oppelt,[1] Daniele Sertore,[4] Frank Stephan,[1] Reza Valizadeh,[3] Grygorii Vashchenko,[1] and Tobias Weilbach[1]

AFFILIATIONS

[1]Deutsches Elektronen-Synchrotron DESY, 15738 Zeuthen, Germany
[2]Deutsches Elektronen-Synchrotron DESY, 22607 Hamburg, Germany
[3]ASTeC, STFC Daresbury Laboratory, Daresbury, Warrington, WA4 4AD Cheshire, United Kingdom
[4]Istituto Nazionale di Fisica Nucleare, 20133 Milano, Italy

[a)]**Present address:** Deutsches Elektronen-Synchrotron DESY, 22607 Hamburg, Germany.
[b)]**Authors to whom correspondence should be addressed:** gregor.loisch@desy.de and ye.lining.chen@desy.de

ABSTRACT

Electron photoinjectors provide high-brightness electron beams to numerous research applications in physics, chemistry, material, and life sciences. Semiconductor photocathodes are widely used here, as they enable the production of low-emittance beams with variable charge at high repetition rates. One of the key figures of merit of photocathodes is the minimum achievable bunch length. In semiconductor cathodes, this is dominated by scattering effects and varying penetration depths of the extracting photons, which leads to a characteristic electron emission function. We present a method to determine this cathode time response with resolution on the tens of femtoseconds level, breaking the resolution barrier encountered in previous studies. The method is demonstrated with cesium-telluride (Cs_2Te) and gold cathodes, revealing response times of (184 ± 41) fs up to (253 ± 58) fs for the semiconductor and an upper limit of (93 ± 17) fs for the metal. Monte Carlo simulations of Cs_2Te emission benchmarked to these results give detailed information about the cathode material.

High-gradient, high-brightness photoinjectors[1] are an enabling technology for research fields such as ultrafast electron diffraction (UED),[2] free-electron laser (FEL) science,[3–7] and novel particle accelerators.[8–11] These electron sources are based on emission of low emittance[12] beams from a photocathode by a laser pulse. By placing this cathode inside a radio frequency (RF) accelerating cavity, the photoelectron gun, the electrons are accelerated with accelerating fields of tens of MV/m immediately after emission. To efficiently extract photoelectrons, laser pulses of usually UV light are shone on cathodes made of metal or semiconductors. In photoinjector physics and in this manuscript, semiconductor refers to semiconductor materials in which the dominant scattering process during photoemission is electron-phonon scattering. These allow for very high photon to electron conversion rates, i.e., quantum efficiencies (QEs) of up to tens of percent, which enables the extraction of high average currents with moderate size laser systems, while metal cathodes exhibit typical QE values on the order of only 10^{-4}.

Aside from QE, another key parameter of the cathodes is the length of the extracted electron bunch compared to the incoming laser pulse.[13] At high charge densities, this is dominated by bunch lengthening due to Coulomb repulsion between the particles at low energies. At low charge densities and high fields at extraction, the bunch length is defined by the emission process from the cathode. Whereas in metal cathodes only electrons excited at a depth of a few to few tens of nanometers can escape the material, electrons excited in a semiconductor cathode can still escape from depths of several hundred nanometers. Such electrons have to travel a distance corresponding to the photon penetration depth back to the surface, where they can be emitted.[14] On this path, they are scattered off, e.g., lattice phonons. These two statistical processes, varying photon penetration depths and electron scattering in the semiconductor, lead to a difference in the delay between the photon arrival at the cathode and emission of an electron excited by this photon from the cathode. In an ensemble of photons—and consequently, in the ensemble of released electrons—the statistical

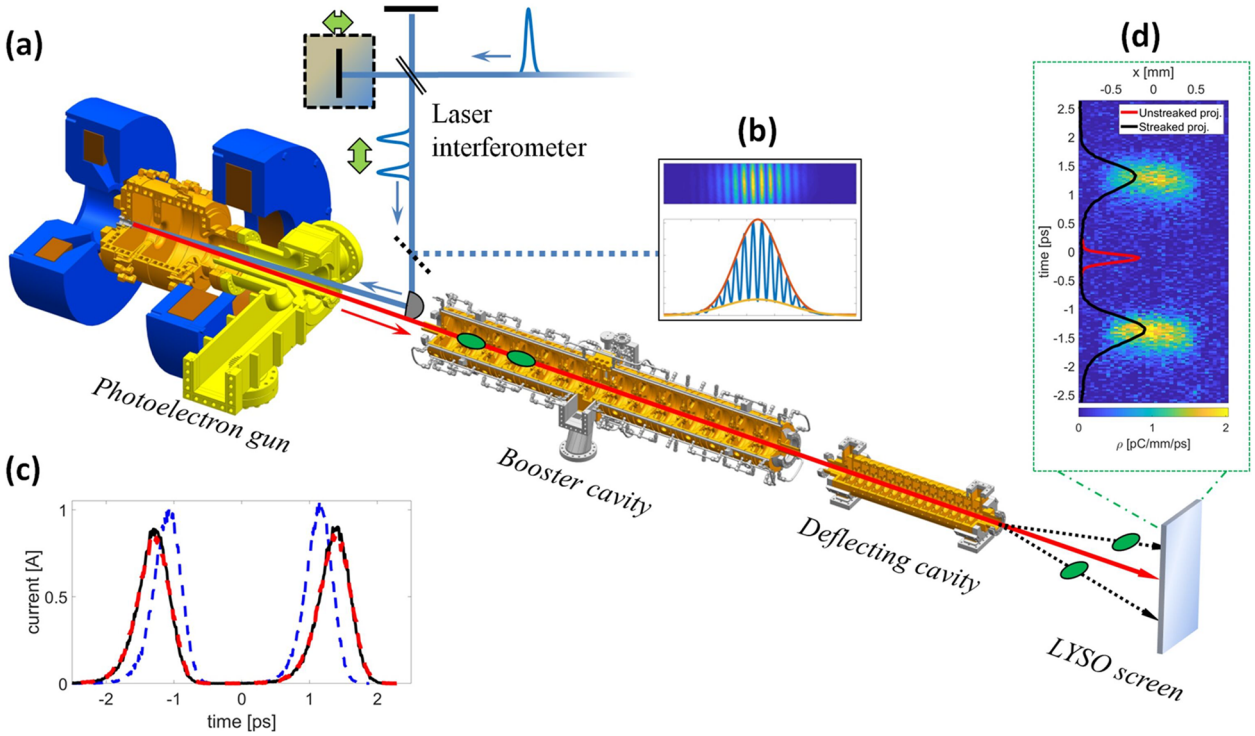

FIG. 1. Schematic measurement setup (not to scale) for femtosecond photocathode time response measurements (a) with an excerpt from laser interferometry measurements (b) and the simulated evolution of the longitudinal bunch profiles from extraction (black line) to measurement position (blue dashed line) to simulated reconstruction of the input profile (red dashed line) (c). An example of a measured transverse-longitudinal bunch projection is shown in (d) with normalized projections on the time axis for the deflected and non-deflected bunches in black and red, respectively.

variation in this delay causes lengthening of the extracted electron bunch with respect to the original light pulse.[15] This lengthening is a fundamental property of the cathode material. The shape of the emission curve will here be called the cathode response function and its characteristic time constant will be referred to as the cathode response time. Retardation of bunch emission with respect to the arrival time of the extracting laser pulse (i.e., the average delay between photon arrival and emission) will not be considered here.

Modeling of the emission process of electrons from a cathode requires detailed knowledge of its properties. Therefore, measuring the cathode time response is a further step toward accurate modeling of any electron source based on photoemission. This knowledge is also especially important for photocathode-laser-based bunch shaping,[16–19] manipulation of the bunch charge distribution at the photocathode,[20–22] ultra-short bunch applications like advanced UED setups,[23,24] or novel FEL schemes.[25]

Cesium telluride (Cs_2Te)[26–31] is one of the most widely used semiconductor materials in photoinjectors.[7,32–41] Several calculations of emission from Cs_2Te have been published,[15,42,43] and also experiments have been performed to determine the time response of this material[27,28,44] as well as of others.[45,46] The experiments employed a streak camera, energy spectrum analysis, and an RF-deflector to resolve the temporal distribution of electron bunches extracted from semiconductor cathodes. Yet, due to insufficient time resolution, the experimental studies were only able to set an upper limit to the timescale of the cathode response but could not verify the predicted response function, nor determine the response time. In this Letter, we describe a method to measure the time response of any photoemissive material compatible with vacuum and high electric field conditions in a photoelectron gun with resolution down to a few ten femtoseconds and demonstrate its applicability by measuring the cathode response function and time of Cs_2Te and gold.

The measurement method is based on precise measurement of the extracted electron bunches' longitudinal profiles. A schematic of the measurement setup at the Photo Injector Test Facility at DESY in Zeuthen (PITZ)[47,48] is shown in Fig. 1(a): A UV laser pulse is sent into a Michelson interferometer, where it is split into two pulses that travel collinearly (blue line). By adjusting the length of one of the two interferometer arms, the delay between the two laser pulses can be controlled. The two pulses are then transported to the photocathode, which is placed at the backplane of a 1.3 GHz normal-conducting RF-gun on a cathode plug made of molybdenum, exchangeable via a load-lock system. Here, they extract two electron bunches with a longitudinal profile corresponding to the longitudinal profile of the laser pulses, convoluted with the cathode time response function [Fig. 1(a), green dots, red line]. The mode-locked ytterbium frontend laser is set to full compression by maximizing the pulse energy of the UV laser pulses, which are generated in two consequent frequency-doubling stages with a final central wavelength of 257 nm. A Gaussian function is used to represent the longitudinal laser pulse shape.

Relative positions of the mirrors in the laser interferometer are measured via field autocorrelation by tilting one of the interferometer mirrors by 40 μrad and observing the interference of the two laser pulses while changing their delay on a charge coupled device (CCD) camera. Equal arm length in the interferometer is determined by finding the maximum difference between minimum and maximum intensities in the interference pattern [shown in Fig. 1(b), orange and red fit lines]. By the relative mirror position to equal arm length, the delay of the laser pulses can be adjusted. For measurements shown here, a relative mirror position of 0.4 mm (i.e., a relative path length difference of 0.8 mm) was used, resulting in a laser pulse delay of 2.667 ps. The longitudinal profile of the cathode laser pulse was measured using a transient-grating (TG) technique,[49] which revealed a temporal Gaussian shape with an RMS length of (113 ± 7) fs. The transverse laser spot size on the cathode was 4 mm.

Photocathodes made of Cs_2Te are produced by subsequent deposition of the two materials onto a polished molybdenum plug surface: first, a layer of Te is deposited with a thickness of 10 nm, determined by the deposition rate and duration.[30] Subsequently, Cs is deposited while monitoring the QE until a maximum is reached. The metal cathode was produced by magnetron-sputtering a gold film onto a polished Mo plug.

After extraction of the bunches from the photocathode, they are accelerated in the standing-wave RF-gun and the downstream RF booster cavity, phased such that they acquire the maximum mean momenta of 6.7 and 22 MeV/c, respectively. A third, traveling-wave RF-cavity, operating at 3 GHz, accelerates the bunches transversely with a maximum gradient of 1.8 MV/m [Fig. 1(a), black dotted lines]. Setting the bunches close to the zero-crossing of the field in this transverse deflecting structure (TDS)[50–52] allows measurement of the temporal profile of the electron bunches on a downstream cerium-doped lutetium yttrium orthosilicate scintillator (LYSO) screen using a CCD camera. Bunches are focused onto this screen using two quadrupole magnets positioned between booster and TDS cavities. An example of a measured transverse-longitudinal projection of the bunches is depicted in Fig. 1(d).

Due to phase slippage at low energies, the bunches are slightly compressed until they reach the position of the TDS. This can be seen in Fig. 1(c), where the longitudinal profile of the two bunches at extraction (black solid line) and the profile at the measurement position (blue dashed line) as simulated in ASTRA[53] are shown. To overcome the effect of this compression on the measured profile, the time axis of the TDS measurement is defined by setting the separation of the bunches on the measurement screen equal to the relative path length difference of the photocathode laser pulses in the interferometer. The profile reconstructed using this method—simulation of which is shown in Fig. 1(c), red dashed line—resembles the profile at the cathode (black line) accurately.

Transverse-longitudinal correlations in the individual bunches or the bunch pair, as well as interferometer mirror position errors due to the mirror tilt for relative path length measurement can cause systematic errors in the measurement on the order of tens of femtoseconds. To mitigate these errors, measurements are conducted on both zero crossing phases of the deflecting field in the TDS as well as with the relative mirror position in the interferometer changed to the opposite path length difference. By averaging over all these measurements, the systematic uncertainty on the longitudinal bunch profile measurement can, in principle, be reduced to the resolution of the TDS measurement, which is given by the transverse bunch size of the unstreaked beam [see Fig. 1(b), red line] and is in the PITZ setup on the order of 45 fs root mean square (RMS) at the used bunch energy and laser spot size on the cathode, which was optimized here to minimize space charge effects. It should be noted that the transverse bunch profile is usually close to Gaussian and, therefore, does not deteriorate asymmetric functions that it is convoluted with but only contributes to the timescale of the symmetric part of the measured bunch profile. The expected exponential response function is hence not modified by this.

Applying the measurement method described above, the time response of various photocathodes has been measured at PITZ. To determine the characteristic cathode response function of semiconductor materials, bunches extracted from well understood metal cathodes[54] have been measured as a reference. Figure 2(a) shows an example of the longitudinal bunch profiles measured for a gold cathode. The mean profile (red solid line) of 40 consecutive shots (green dots) is fitted with a Gaussian function, as expected from the laser longitudinal pulse shape, and the error mitigation procedure described above is applied. A Gaussian RMS length of (183 ± 10) fs is found for the gold emission data, and the RMS error of the fits is 0.59 mA. In Fig. 2(b), similar traces are depicted for a beam extracted from a Cs_2Te cathode. Here, mean bunch shapes were fitted using a Gaussian convoluted with an exponential function. This exponential contribution to the bunch profile, which is merely present in the case of the gold metal cathode, is also predicted to be the characteristic response of Cs_2Te in simulations.[43,55] Again, good agreement can be seen with significant exponential time constant at the bunch tail. The error mitigation procedure reveals an exponential time constant of (184 ± 42) fs and a Gaussian contribution of (193 ± 17) fs RMS, at an RMS fit error of 0.47 mA. Fitting with a Gaussian function results in a nearly doubled RMS fit error of 0.8 mA. When applying a Gaussian-exponential fit to the gold cathode data, an exponential time constant of (93 ± 17) fs is found at an RMS fit error of 0.64 mA, which is similar to the error of the pure Gaussian fit. Therefore, the measured value is considered to be close to the resolution limit for the exponential response time at the used experimental parameters (laser pulse shape, screen material, bunch charge, streaking strength, etc.) and to represent a first upper limit for the response time of gold. One possible reason for such a time constant if it was confirmed in future measurements—which would be rather long compared to the expected response time of metals in the 10 fs range—is surface roughness, which will be the subject of future work. Figure 2(c) illustrates the difference between bunch shapes extracted from metal and semiconductor cathodes.

Measurements with different bunch charges up to (2.66 ± 0.50) pC total charge showed similar Gaussian and exponential time constants, which implies negligible influence of space charge forces on the bunch shape. Furthermore, measurements with different maximum field gradients at the cathode of down to 45 MV/m have been performed, showing no change in the measured cathode response. This might allow for increasing the TDS resolution by optimization of, e.g., bunch energy in future studies. Measurement errors are dominated by statistical variations, mostly due to rather low signal to noise ratios at the low bunch charges.

The Cs_2Te cathode used in the measurement shown in Fig. 2(b) had been used for electron bunch production at PITZ for more than one year with several intermediate storage periods under ultra-high

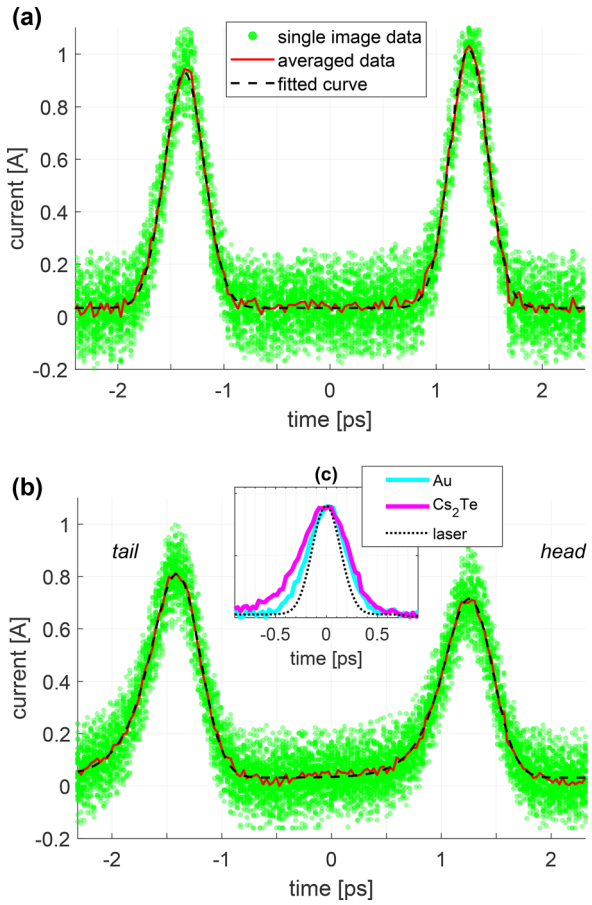

FIG. 2. Bunch current profiles of 40 consequent bunch pairs extracted from gold (a) and Cs_2Te (b) photocathodes. Traces were centered to the same peak current positions, and the average waveform was fitted with a sum of two Gaussian functions (a) and a sum of two Gaussian functions, each convoluted with an exponential decay (b). Plots (a) and (b) share the same bunch orientation and trace coloring. Average total charges of the bunches were (1.09 ± 0.19) pC in (a) and (1.02 ± 0.49) pC in (b). Inset (c) shows an overlay of normalized and centered bunch current profiles extracted from gold and Cs_2Te cathodes as well as the normalized photocathode laser pulse profile acquired from TG measurements, convolved with the TDS resolution and the expected pulse lengthening due to group velocity dispersion in the beamline to the photocathode.

vacuum conditions. Directly after first insertion into the gun, the quantum efficiency was measured to be 12.45% at a maximum field gradient of 60 MV/m. At the time of the response time measurements, the QE had dropped to (7.0 ± 0.4)%. For comparison, a Cs_2Te cathode produced in the same setup at DESY Hamburg under the same conditions was inserted and conditioned in the PITZ gun. At first usage, the exponential cathode response time was measured to be (184 ± 41) fs at a total bunch charge of (1.04 ± 0.44) pC. Its measured QE was (9.1 ± 0.5)%. Another previously unused cathode, produced with a similar procedure in a similar setup at INFN Milano, Italy, was finally inserted into the PITZ photoelectron gun. This cathode's exponential response time was measured to be (253 ± 58) fs at (0.98 ± 0.48) pC, and its QE was (23.4 ± 1.4)%.

Monte Carlo calculations have been performed to verify that theoretical predictions conformed to the measured cathode responses and quantum efficiencies. The cathode material is treated here as a homogeneous body, thus giving average parameter values for all different, polycrystalline structures that are present in the investigated cathodes. These calculations are based on 1-to-1 photoemission according to Spicer's three-step model.[14] Initial electron excitation conditions are derived from density of states according to Refs. 42 and 56. The considered room temperature work function of Cs_2Te is decomposed into the fixed bandgap (3.3 eV) and variable electron affinity. Electron-phonon scattering is assumed to be the dominating scattering process with a mean free path (MFP) of 1.6 nm and a mean energy loss per collision of 4 meV.[15,43] Upon exit of the cathode surface, emission angle dependency is taken into account. Every simulation result is achieved from 200 simulations with 150 000 particles each.

Simulated and measured response times and quantum efficiencies are summarized in Fig. 3. An exponential time response is observed in these simulations, similar to experiment. To achieve the measured cathode parameters of the used DESY-type cathode, an electron affinity of 0.36 eV is used. Slight modification of this value to 0.34 eV allows it to shift the QE to reproduce the measured values of the fresh DESY-type cathode, while maintaining a similar response time. This is compatible with the assumption that during cathode aging, surface conditions change, which is represented by the electron affinity. Reproducing the measured parameters of the INFN-type cathode requires an electron affinity of 0.257 eV and a modification of the mean free path to 1.3 nm. Similar agreement can be achieved by, e.g., varying the cathode thickness instead of the mean free path. Nevertheless, all simulation parameters that were used to achieve agreement between model and measurement results are in line with previously reported values,[43,57,58] which confirms the general validity of the used model and suggest that this benchmarking can be used to determine material parameters by measuring the response time. Further investigations are needed to clarify how and why the two cathode types are different, despite similar production procedures.

In summary, we presented a method to measure the time response of photocathodes in RF-photoelectron guns and demonstrated its validity by measuring shape and time constant of the Cs_2Te

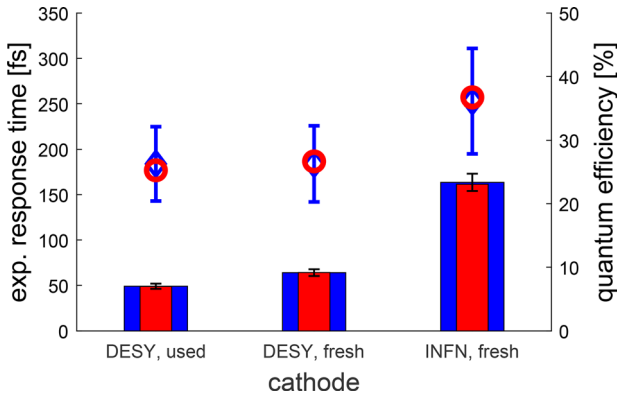

FIG. 3. Measured and simulated exponential response times and QE's for different Cs_2Te cathodes. Markers show response times, and bars show quantum efficiencies. Blue color corresponds to measurements and red to simulated results.

photocathode time response, which could previously only be estimated to be on a timescale of around 400 fs.[36] This method differs from previous approaches by operating in a regime of significantly higher acceleration gradients and by rigorous error mitigation. The longitudinal shape of electron bunches extracted from the cathode is measured by means of a transverse RF-deflector. The measured Cs_2Te cathodes show exponentially decaying electron emission with time constants of (184 ± 42) fs up to (253 ± 58) fs, depending on the exact setup and procedure of production, as so far all cathodes produced at the same institute with the same procedure also exhibit similar response times. Monte Carlo simulations were benchmarked with these results and could reproduce the measured shape and timescale of the emission process as well as the measured quantum efficiencies. For electron emission from gold, a response time of (93 ± 17) fs was measured, which represents a first, upper limit for the response time of metal cathodes.

Knowledge of the exact time response of photocathodes will allow one to check and ultimately optimize their compatibility with applications requiring short response times like femtosecond ultrafast electron diffraction[23] or novel, short bunch free-electron laser schemes[25] as well as with applications requiring longer response times.[22] This might open up new operation modes and also improve the performance of existing facilities.

Future studies and simulations along with, e.g., x-ray spectroscopy measurements may also reveal fundamental properties of different photoemitting materials.[59] In the field of photoinjectors, these studies will enable more complete modeling of the emission process, which is critical for the achieved bunch quality. Further work will concentrate on different cathode thicknesses, deposition techniques, and also other cathode materials like Cs_2KSb and Cu, while further improving our measurement resolution by optimizing the streaking strength, laser pulse length, and signal to noise ratio.

AUTHOR DECLARATIONS

Conflict of Interest

The authors have no conflict of interest to disclose.

DATA AVAILABILITY

The data that support the findings of this study are available from the corresponding authors upon reasonable request.

REFERENCES

[1]B. E. Carlsten, "New photoelectric injector design for the Los Alamos National Laboratory XUV FEL accelerator," Nucl. Instrum. Methods Phys. Res., Sect. A **285**, 313–319 (1989).

[2]A. H. Zewail, "4D ultrafast electron diffraction, crystallography, and microscopy," Annu. Rev. Phys. Chem. **57**, 65–103 (2006).

[3]W. Ackermann, G. Asova, V. Ayvazyan *et al.*, "Operation of a free-electron laser from the extreme ultraviolet to the water window," Nat. Photonics **1**, 336–342 (2007).

[4]P. Emma, R. Akre, J. Arthur *et al.*, "First lasing and operation of an ångstrom-wavelength free-electron laser," Nat. Photonics **4**, 641–647 (2010).

[5]C. Milne, T. Schietinger, M. Aiba *et al.*, "SwissFEL: The Swiss X-ray free electron laser," Appl. Sci. **7**, 720 (2017).

[6]H.-S. Kang, C. K. Min, H. Heo *et al.*, "Hard x-ray free-electron laser with femtosecond-scale timing jitter," Nat. Photonics **11**, 708–713 (2017).

[7]W. Decking, S. Abeghyan, P. Abramian *et al.*, "A MHz-repetition-rate hard x-ray free-electron laser driven by a superconducting linear accelerator," Nat. Photonics **14**, 391–397 (2020).

[8]R. D'Arcy, A. Aschikhin, S. Bohlen *et al.*, "FLASHForward: Plasma-wakefield accelerator science for high-average-power applications," Philos. Trans. R. Soc. A **377**, 20180392 (2019).

[9]V. Yakimenko *et al.*, "FACET-II facility for advanced accelerator experimental tests," Phys. Rev. Accel. Beams **22**, 101301 (2019).

[10]U. Dorda, R. Assmann, R. Brinkmann *et al.*, "SINBAD—The accelerator R&D facility under construction at DESY," Nucl. Instrum. Methods Phys. Res., Sect. A **829**, 233–236 (2016).

[11]P. Londrillo, P. Gatti, and M. Ferrario, "Numerical investigation of beam-driven PWFA in quasi-nonlinear regime," Nucl. Instrum. Methods Phys. Res., Sect. A **740**, 236–241 (2014).

[12]E. D. Courant and H. S. Snyder, "Theory of the alternating-gradient synchrotron," Ann. Phys. **3**, 1–48 (1958).

[13]N. Moody, K. L. Jensen, A. Shabaev *et al.*, "Perspectives on designer photocathodes for x-ray free-electron lasers: Influencing emission properties with heterostructures and nanoengineered electronic states," Phys. Rev. Appl. **10**, 047002 (2018).

[14]W. E. Spicer, "Photoemissive, photoconductive, and optical absorption studies of alkali-antimony compounds," Phys. Rev. **112**, 114 (1958).

[15]W. E. Spicer and A. Herrera-Gómez, "Modern theory and applications of photocathodes," Proc. SPIE **2022**, 18–33 (1993).

[16]P. Michelato, "Photocathodes for RF photoinjectors," Nucl. Instrum. Methods Phys. Res., Sect. A **393**, 455–459 (1997).

[17]I. Will and G. Klemz, "Generation of flat-top picosecond pulses by coherent pulse stacking in multicrystal birefringent filter," Opt. Express **16**, 14922 (2008).

[18]F. Lemery and P. Piot, "Tailored electron bunches with smooth current profiles for enhanced transformer ratios in beam-driven acceleration," Phys. Rev. Spec. Top. –Accel. Beams **18**, 081301 (2015).

[19]G. Loisch, G. Asova, P. Boonpornprasert *et al.*, "Observation of high transformer ratio plasma wakefield acceleration," Phys. Rev. Lett. **121**, 064801 (2018).

[20]O. J. Luiten, S. B. Van der Geer, M. J. De Loos *et al.*, "How to realize uniform three-dimensional ellipsoidal electron bunches," Phys. Rev. Lett. **93**, 094802 (2004).

[21]P. Musumeci, J. T. Moodi, R. J. England *et al.*, "Experimental generation and characterization of uniformly filled ellipsoidal electron-beam distributions," Phys. Rev. Lett. **100**, 244801 (2008).

[22]S. Bettoni, M. C. Divall, R. Ganter *et al.*, "Impact of laser stacking and photocathode materials on microbunching instability in photoinjectors," Phys. Rev. Accel. Beams **23**, 024401 (2020).

[23]F. Qi, Z. Ma, L. Zhao *et al.*, "Breaking 50 femtosecond resolution barrier in MeV ultrafast electron diffraction with a double bend Achromat compressor," Phys. Rev. Lett. **124**, 134803 (2020).

[24]S. Karkare, L. Boulet, L. Cultrera *et al.*, "Ultrabright and ultrafast III–V semiconductor photocathodes," Phys. Rev. Lett. **112**, 097601 (2014).

[25]J. Rosenzweig, D. Alesini, G. Andonian *et al.*, "Generation of ultra-short, high brightness electron beams for single-spike SASE FEL operation," Nucl. Instrum. Methods Phys Res., Sect. A **593**, 39–44 (2008).

[26]E. Chevallay, J. Durand, S. Hutchins *et al.*, "Photocathodes tested in the dc gun of the CERN photoemission laboratory," Nucl. Instrum. Methods Phys. Res., Sect. A **340**, 146–156 (1994).

[27]R. Bossart, H. Braun, F. Chautard *et al.*, "CLIC test facility developments and results," in *Proceedings Particle Accelerator Conference, Dallas* (IEEE Press, 1995), pp. 719–721.

[28]S. H. Kong, J. Kinross-Wright, D. C. Nguyen, and R. L. Sheffield, "Cesium telluride photocathodes," J. Appl. Phys. **77**, 6031 (1995).

[29]A. Fry, E. Hahn, W. Hartung *et al.*, "Experience at Fermilab with high quantum efficiency photo-cathodes for rf electron guns," in *Proceedings of the XIX International Linac Conference, TU4101*, Chicago (National Technical Information Service NTIS, U.S. Department of Commerce, 1998), pp. 642–644, available at https://accelconf.web.cern.ch/l98/Proceedings.html.

[30]D. Sertore, S. Schreiber, K. Floettmann *et al.*, "First operation of cesium telluride photocathodes in the TTF injector RF gun," Nucl. Instrum. Methods Phys. Res., Sect. A **445**, 422–426 (2000).

[31]J. P. Hartung, W. Carneiro, D. Edwards *et al.*, "Studies of photo-emission and field emission in an rf photo-injector with a high quantum efficiency photocathode," in *Proceedings of the Particle Accelerator Conference WPAH063, Chicago* (IEEE Press, 2001), pp. 2239–2241.

[32]S. Schreiber, "Soft and hard x-ray SASE free electron lasers," Rev. Accel. Sci. Technol. **03**, 93–120 (2010).
[33]S. Lederer, F. Brinker, and S. Schreiber, "Update on the photocathode lifetime at FLASH and European XFEL," in Proceedings of the 39th International Free Electron Laser, Hamburg, Germany, http://www.jacow.org, pp. 427–429.
[34]C. Hessler, E. Chevallay, M. Divall Csatari *et al.*, "Lifetime studies of Cs_2Te cathodes at the PHIN RF photoinjector at CERN," in Proceedings of the 3rd International Particle Accelerator Conference, New Orleans, TUPPD066, 2012.
[35]K. Hirano, M. Fukuda, M. Takano *et al.*, "High-intensity multi-bunch beam generation by a photo-cathode RF gun," Nucl. Instrum. Methods Phys. Res., Sect. A **560**, 233–239 (2006).
[36]A. Aryshev, Y. Honda, K. Lekomtsev *et al.*, "Cs_2Te photocathode response time measurements and femtosecond comb electron beam generation as a milestone towards pre-bunched THz FEL realization," in Proceedings of the 7th International Particle Accelerator Conference, Busan, THPOW007, 2016.
[37]M. Gaowei, J. Sinsheimer, D. Strom *et al.*, "Codeposition of ultrasmooth and high quantum efficiency cesium telluride photocathodes," Phys. Rev. Accel. Beams **22**, 073401 (2019).
[38]H. Panuganti and P. Piot, "Observation of two-photon photoemission from cesium telluride photocathodes excited by a near-infrared laser," Appl. Phys. Lett. **110**, 093505 (2017).
[39]J. Dai, Q. Sheng-Wen, C. Cheng *et al.*, "Cs_2Te photocathode fabrication system at Peking University," Chin. Phys. C **36**, 475–478 (2012).
[40]E. Prat, S. Bettoni, H. H. Braun *et al.*, "Measurements of copper and cesium telluride cathodes in a radio-frequency photoinjector," Phys. Rev. Spec. Top. –Accel. Beams **18**, 043401 (2015).
[41]L. Zheng, J. Shao, E. E. Wisniewski *et al.*, "Rapid thermal emittance and quantum efficiency mapping of a cesium telluride cathode in an rf photoinjector using multiple laser beamlets," Phys. Rev. Accel. Beams **23**, 052801 (2020).
[42]R. A. Powell, W. E. Spicer, G. B. Fisher *et al.*, "Photoemission studies of cesium telluride," Phys. Rev. B **8**, 3987 (1973).
[43]G. Ferrini, P. Michelato, and F. Parmigiani, "A Monte Carlo simulation of low energy photoelectron scattering in Cs_2Te," Solid State Commun. **106**, 21–26 (1998).
[44]A. Aryshev, M. Shevelev, Y. Honda *et al.*, "Femtosecond response time measurement of a Cs_2Te photocathode," Appl. Phys. Lett. **111**, 033508 (2017).
[45]I. Bazarov, B. M. Dunham, X. Liu *et al.*, "Thermal emittance and response time measurements of a GaN photocathode," J. Appl. Phys. **105**, 083715 (2009).
[46]L. Cultrera, I. Bazarov, A. Bartnik *et al.*, "Thermal emittance and response time of a cesium antimonide photocathode," Appl. Phys. Lett. **99**, 152110 (2011).
[47]F. Stephan, C. H. Boulware, M. Krasilnikov *et al.*, "Detailed characterization of electron sources yielding first demonstration of European x-ray free-electron laser beam quality," Phys. Rev. Spec. Top. –Accel. Beams **13**, 020704 (2010).
[48]M. Krasilnikov, F. Stephan, G. Asova *et al.*, "Experimentally minimized beam emittance from an L-band photoinjector," Phys. Rev. Spec. Top. –Accel. Beams **15**, 100701 (2012).
[49]J. T. Fourkas and M. D. Fayer, "The transient grating: A holographic window to dynamic processes," Acc. Chem. Res. **25**, 227–233 (1992).
[50]R. H. Miller, R. F. Koontz, and D. D. Tsang, "The SLAC injector," IEEE Trans. Nucl. Sci. **12**, 804 (1965).
[51]M. Röhrs, C. Gerth, H. Schlarb *et al.*, "Time-resolved electron beam phase space tomography at a soft x-ray free-electron laser," Phys. Rev. Spec. Top. –Accel. Beams **12**, 050704 (2009).
[52]H. Huck, P. Boonpornprasert, L. Jachmann *et al.*, "Progress on the PITZ TDS," in International Beam Instrumentation Conference IBIC, Barcelona, Spain, http://www.jacow.org, pp. 744–747.
[53]K. Flöttmann, see http://www.desy.de/~mpyflo/ for "Astra—A space charge tracking algorithm v3.2" (2017).
[54]D. H. Dowell and J. F. Schmerge, "Quantum efficiency and thermal emittance of metal photocathodes," Phys. Rev. Spec. Top. –Accel. Beams **12**, 074201 (2009).
[55]P. Piot, Y.-E. Sun, T. J. Maxwell, J. Ruan, E. Secchi, and J. C. T. Thangaraj, "Formation and acceleration of uniformly filled ellipsoidal electron bunches obtained via space-charge-driven expansion from a cesium-telluride cathode," Phys. Rev. Spec. Top. –Accel. Beams **16**, 010102 (2013).
[56]K. L. Jensen, *Advances in Imaging and Electron Physics: Electron Emission Physics* (Academic Press, New York, 2007).
[57]R. Xiang, A. Arnold, P. Michel *et al.*, "Thermal emittance measurement of the Cs_2Te photocathode in FZD superconducting RF gun," in Free Electron Laser Conference, WEPB22, Malmö, Sweden, http://www.jacow.org, pp. 449–452.
[58]V. Miltchev, J. Baehr, H. J. Grabosch *et al.*, "Measurements of thermal emittance for cesium telluride photocathodes at PITZ," in Free Electron Laser Conference, THPP042, Stanford, CA, http://www.jacow.org, pp. 560–563.
[59]W. E. Spicer, "The use of photoemission to determine the electronic structure of solids," J. Phys. Colloq. **34**, C6-19 (1973).